

## COMPACT DUAL-BAND REJECTION FILTER BASED ON COMPLEMENTARY MEANDER LINE SPLIT RING RESONATOR

**X. Hu** <sup>†</sup>

Division of Electromagnetic Engineering  
School of Electrical Engineering  
Royal Institute of Technology  
S-100 44 Stockholm, Sweden

**Q. Zhang**

Centre for Optical & Electromagnetic Research  
Zhejiang University  
Hangzhou 310058, China

**S. He** <sup>‡</sup>

Division of Electromagnetic Engineering  
School of Electrical Engineering  
Royal Institute of Technology  
S-100 44 Stockholm, Sweden

**Abstract**—In this paper, a complementary meander line split-ring resonator (C-MLSRR) model is proposed, and its equivalent circuit model is given. Prototypes of microstrip lines loaded with C-MLSRR with and without series capacitive gaps are designed, which exhibit a negative permittivity behavior (without series capacitive gaps) and a left-handed behavior (with series capacitive gaps), respectively, at two different frequencies. The application of the C-MLSRRs in compact dual band (i.e., 2.52 GHz and 5.35 GHz) notch filter for wideband application is presented to highlight the unique features of the C-MLSRRs.

---

Corresponding author: X. Hu (xinhu@kth.se).

<sup>†</sup> This author is also with Centre for Optical & Electromagnetic Research, Zhejiang University, Hangzhou 310058, China.

<sup>‡</sup> This author is also with Centre for Optical & Electromagnetic Research, Zhejiang University, Hangzhou 310058, China.

## 1. INTRODUCTION

The possibility to obtain media with simultaneously negative permeability and permittivity (also called left-handed metamaterials (LHMs)) was firstly hypothesized by Veselago in the late 60s [1]. The first experimental evidence of such a medium was demonstrated [2], which consisted of a bulky combination of metal wires and Split Ring Resonators (SRRs). The electromagnetic properties of the SRR [3, 4] show that by virtue of the distributed capacitance between concentric rings and overall ring inductance, SRR behaves as an LC resonant tank that can be excited by an external magnetic flux. Thereafter, another key particle has been proposed for metamaterial design [5], namely, the complementary split-ring resonator (CSRR), which is the negative image of an SRR. The authors have demonstrated that CSRRs etched in the ground plane of planar transmission media provide a negative effective permittivity to the structure. Since SRRs and CSRRs are both planar configurations, SRRs and CSRRs (properly combined with shunt metallic wires or series gaps) have been successfully applied to the design of novel planar microwave circuit and devices [6–11] based on the equivalent circuit model [5].

In this paper, a meander line SRR (MLSRR) model and its complementary structure (C-MLSRR) are proposed and analyzed. Their equivalent circuit models are given. As C-MLSRR has two resonant frequencies, the transmission line loaded with CML-SRR can be used to reject unwanted frequencies as a dual bandstop filter.

## 2. COMPLEMENTARY MEANDER LINE SPLIT RING RESONATOR (C-MLSRR)

The topology of the MLSRR (shown in Fig. 1) is essentially the same as that of the single SRR [12]. However, the line connect the split is replaced with a meander line. Fig. 1(a) shows the topology of MLSRR and its equivalent circuit model. The meander line is modeled as a parallel connected inductance  $L_M$  and capacitance  $C_M$ , which represents the electrical coupling between the meander lines.  $C_S$  stands for the capacitance between the split, and  $L_S$  is the inductance of the lines connected with the split.

Due to the duality of the geometries of MLSRR and C-MLSRR, we can derive the equivalent circuit model of C-MLSRR (shown in Fig. 1(b)). In this figure, we can see the C-MLSRR has two different resonant frequencies:

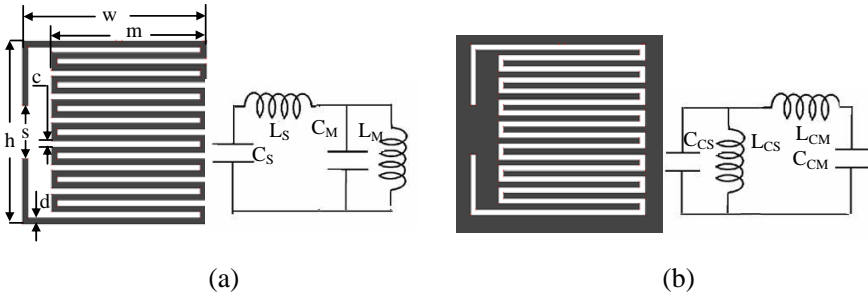


**Figure 1.** Geometry of (a) MLSRR and (b) C-MLSRR, and their equivalent circuits. Gray area represents the metallization.

$$\begin{aligned} \omega_1 &= 2\pi f_1 \\ &= \frac{(L_{CS}C_{CS} + L_{CM}C_{CM} + L_{CS}C_{CM})}{-\sqrt{(L_{CS}C_{CS} + L_{CM}C_{CM} + L_{CS}C_{CM})^2 - 4L_{CS}C_{CS}L_{CM}C_{CM}}} \\ \omega_2 &= 2\pi f_2 \\ &= \frac{(L_{CS}C_{CS} + L_{CM}C_{CM} + L_{CS}C_{CM})}{+\sqrt{(L_{CS}C_{CS} + L_{CM}C_{CM} + L_{CS}C_{CM})^2 - 4L_{CS}C_{CS}L_{CM}C_{CM}}} \end{aligned} \quad (1)$$

### 3. MICROSTRIP LINE LOADED WITH C-MLSRR

Let us now focus on finding the equivalent-circuit model corresponding to transmission-line structures loaded with C-MLSRR. The microstrip line loaded with C-MLSRR on the back substrate side is shown in Fig. 2(a). Due to the small electrical dimensions of C-MLSRR at resonance, the structure can be described by means of lumped-element equivalent circuits, and the proposed equivalent-circuit model is shown in Fig. 2(b) [7].  $L$  and  $C$  are the per-section inductance and capacitance of the host transmission line, while the C-MLSRR is electrically coupled with the microstrip line through  $C_M$ .

The equivalent impedance of the parallel branch can be simplified to that shown in the circuit of Fig. 2(c) [17, 18], where

$$L'_{CS} = \frac{C_{CS}}{\omega^2 C_M^2}; C'_{CS} = L_{CS} \omega^2 C_M^2; L'_{CM} = \frac{C_{CM}}{\omega^2 C_M^2}; C'_{CM} = L_{CM} \omega^2 C_M^2 \quad (2)$$

From the circuit of Fig. 2(c), the dispersion relation of C-MLSRR

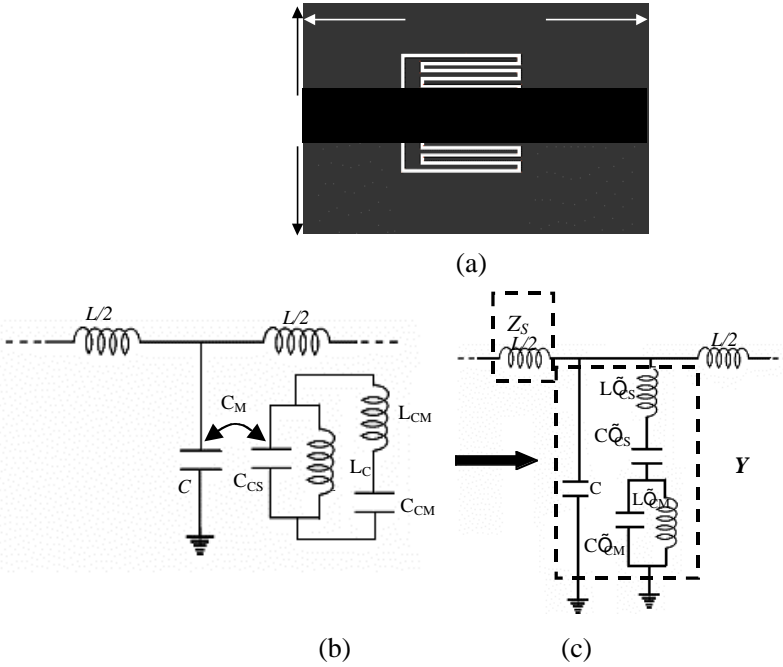


**Figure 2.** Layout of a C-MLSRR loaded microstrip line, (b) its equivalent circuit and (c) its simplified equivalent circuit.

periodically loaded transmission lines can be easily obtained as follows:

$$\cos(\beta l) = 1 - \frac{\omega^2 L}{2} \left[ C + C'_{CS} \frac{1 - \omega^2 L'_{CM} C'_{CM}}{(1 - \omega^2/\omega_1^2)(1 - \omega^2/\omega_2^2)} \right] \quad (3)$$

$\beta$  is the propagation constant for Bloch waves, and  $l$  is the period of the structure. Eq. (3) indicates the presence of two frequency gaps in the vicinity of the two different resonant frequencies, i.e.,  $\omega_1$  and  $\omega_2$ , where the total parallel impedance  $Y$  is highly inductive. These stopbands can be interpreted as due to the presence of negative values for effective  $\epsilon$  [6, 7].

In view of the model, three characteristic frequencies can be identified: the two frequencies that null the shunt impedance (transmission zero frequencies,  $f_1$  and  $f_2$ ) and the intrinsic resonant frequencies of  $L'_{CS}$ , and  $C'_{CS}$ ,  $f_0$ . At  $f_0$  the shunt admittance composed by  $L'_{CS}$ ,  $C'_{CS}$ ,  $L'_{CM}$ , and  $C'_{CM}$  is zero, and the magnitude of the reflection coefficient  $S_{11}$  shows the minimum. These frequencies can

be given by the following equations:

$$f_1^2 = \left(\frac{\omega_1}{2\pi}\right)^2 \frac{(L'_{CS}C'_{CS} + L'_{CM}C'_{CM} + L'_{CS}C'_{CM})}{-\sqrt{(L'_{CS}C'_{CS} + L'_{CM}C'_{CM} + C'_{CS}L'_{CM})^2 - 4L'_{CS}C'_{CS}L'_{CM}C'_{CM}}} \quad (4)$$

$$f_2^2 = \left(\frac{\omega_2}{2\pi}\right)^2 \frac{(L'_{CS}C'_{CS} + L'_{CM}C'_{CM} + C'_{CS}L'_{CM})}{-\sqrt{(L'_{CS}C'_{CS} + L'_{CM}C'_{CM} + C'_{CS}L'_{CM})^2 - 4L'_{CS}C'_{CS}L'_{CM}C'_{CM}}} \quad (5)$$

$$f_0 = \frac{1}{2\pi\sqrt{L'_{CS}C'_{CS}}} \quad (6)$$

To retrieve the parameters (i.e.,  $L'_{CS}$ ,  $C'_{CS}$ ,  $L'_{CM}$ , and  $C'_{CM}$ ) in the equivalent circuit in Fig. 2(c), we need an additional condition [20],

$$Z_S Y = -1 \quad \text{at} \quad f_{\pi/2} \quad (7)$$

where  $f_{\pi/2}$  is the frequency where the phase of the transmission coefficient is  $\psi(S_{21}) = \pi/2$ . These frequencies in (4)–(7) can be obtained through full wave simulation or experimentally determined. Thereafter, we can determine the four reactive element values in the shunt impedance  $Y$ .

#### 4. ILLUSTRATIVE RESULTS

To verify the equivalent circuit model, we apply it to the determination of the electrical parameters of the single cell C-MLSRR loaded microstrip line. The microstrip line is implemented on a Taconic RF35 substrate with dielectric constant  $\varepsilon_r = 3.5$ , loss tangent  $\tan \delta = 0.0018$ , and thickness  $h = 0.76$  mm with the substrate size  $L \times H = 25 \times 20$  mm. The width of the upper conductor strip is 1.8 mm of the  $50 \Omega$  microstrip line. The design parameters are  $d = c = 0.2$  mm,  $s = 1.8$  mm,  $h = 6.2$  mm,  $w = 6.3$  mm, and  $m = 5.3$  mm. The simulated transmission response (using IE3D [20] from Zeland) is shown in Fig. 3. Two rejection bands (return loss  $> 10$  dB) are 2.38 GHz~2.66 GHz, and 5.3 GHz~5.4 GHz. The whole structure of C-MLSRR loaded transmission line is  $0.05\lambda_0 \times 0.05\lambda_0$  at the first stopband centre

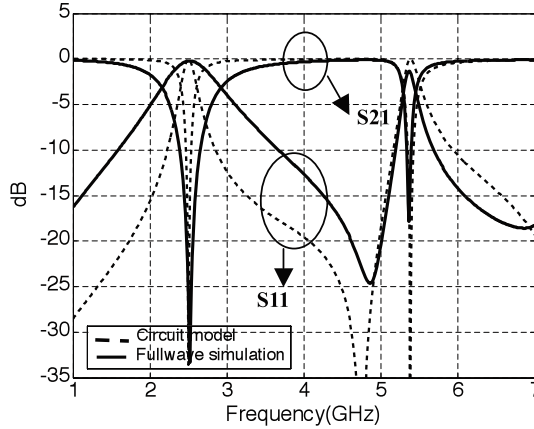


**Figure 3.** Transmission responses of C-MLSRR loaded transmission line. Full wave simulation and equivalent circuit simulation are depicted in bold and dashed lines, respectively.

frequency 2.52 GHz and  $0.11\lambda_0 \times 0.11\lambda_0$  at the second stopband centre frequency 5.35 GHz.

Following the procedures described in the previous section, we can obtain the electrical parameters which are shown in Table 1. The simulated transmission response and transmission coefficients (real part and imaginary part) using full wave simulation and the equivalent circuit model are depicted in Fig. 3 and Fig. 4, which show good verification for the equivalent circuit model in Fig. 2(c).

**Table 1.** Exacted parameters for the structure shown in Fig. 2.

$L'_{CS}$ (H)	$C'_{CS}$ (F)	$L'_{CM}$ (H)	$C'_{CM}$ (F)
$4.5e12/\omega^2$	$\omega^2/12.4e32$	$0.35e12/\omega^2$	$\omega^2/3.58e32$

To tune the stopband center frequencies, we can change the size of the meander line  $w$  and the gap distance  $s$ , and their effects on the center frequencies are shown in Fig. 5.

To achieve a left-handed transmission line we can add capacitive gaps on the top inductor strip of the transmission line [7] as shown in Fig. 6(a). These gaps can provide a negative effective permeability up to a frequency that can be tailored by properly choosing the gap dimensions. If this frequency is set above  $f_1$  and  $f_2$ , the stopbands will switch to passbands in the vicinity of the  $f_1$  and  $f_2$ . The simulated transmission response the C-MLSRR loaded microstrip line with a series gap (with gap width  $g = 0.2$  mm) is shown in Fig. 6(b), where two

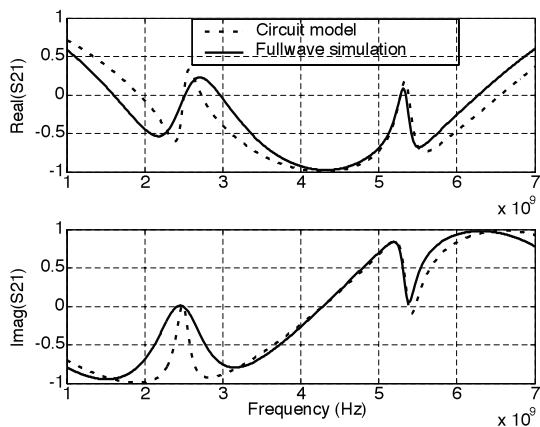


**Figure 4.** Real part and imaginary part of the transmission coefficient  $S_{21}$ .

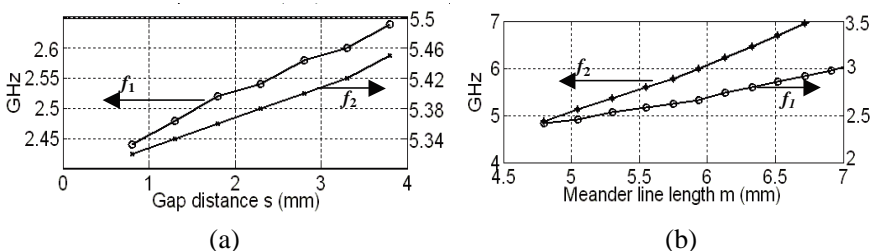


**Figure 5.** Effects on the center frequencies of two rejection bands when C-MLSRR changes (a) gap distance  $s$  and (b) meander line length  $m$ .

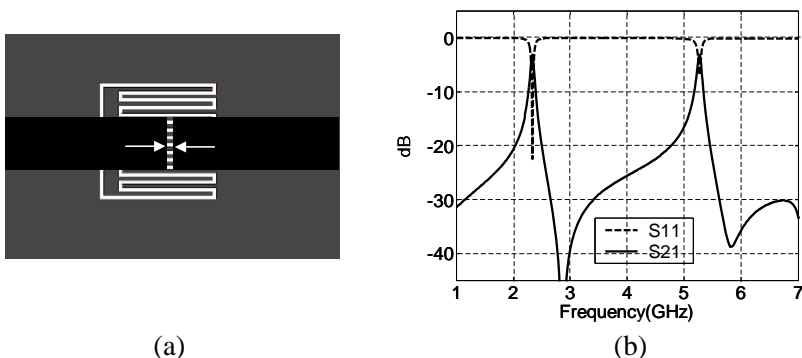


**Figure 6.** (a) Layout of the C-MLSRR loaded microstrip line with a series gap (with gap width  $g = 0.2$  mm) in the upper conductor strip and (b) its simulated transmission response.

transmission peaks appear at 2.4 GHz and 5.3 GHz. This is consistent with the foregoing analysis.

## 5. CONCLUSION

The models of MLSRR and C-MLSRR and their equivalent circuits have been presented. Transmission line loaded with C-MLSRR has shown dual-band rejection, due to the presence of negative permittivity in the vicinity of the two resonate frequencies of C-MLSRR. The method to extract the electrical parameters of the C-MLSRR loaded microstrip line has been presented. From the extracted parameters, very good agreement between the full wave simulation and the equivalent circuit model has been found. It has also been presented that transmission line loaded with C-MLSRR can be changed to be a left-handed transmission line after introducing an effective negative permeability to the transmission line by etching capacitive gap in the conductor strip. This compact design can find applications in filters and rejecting unnecessary frequencies in the wideband applications.

## ACKNOWLEDGMENT

This work was supported by the National Basic Research Program (973) of China (No. 2004CB719802) and the Swedish Research Council (VR) under Project No. 2006-4048.

## REFERENCES

1. Veselago, V. G., "The electrodynamics of substances with simultaneously negative values of  $\epsilon$  and  $\mu$ ," *Soviet Physics Uspekhi*, Vol. 10, 509–514, 1968.
2. Smith, D. R., W. J. Padilla, D. C. Vier, S. C. Nemat-Nasser, and S. Schultz, "Composite medium with simultaneously negative permeability and permittivity," *Physical Review Letters*, Vol. 84, 4184–4187, May 2000.
3. Marqués, R., F. Mesa, J. Martel, and F. Medina, "Comparative analysis of edge and broadside couple split ring resonators for metamaterial design, theory and experiment," *IEEE Trans. Ant. Propag.*, Vol. 51, No. 10, 2572–2581, Oct. 2003.
4. Ran, L. X., J. Huangfu, H. Chen, X. M. Zhang, K.-S. Cheng, T. M. Grzegorzcyk, and J. A. Kong, "Experimental study on several left-handed metamaterials," *Progress In Electromagnetics Research*, PIER 51, 249–279, 2005.

5. Falcone, F., T. Lopetegi, M. A. G. Laso, J. D. Baena, J. Bonache, R. Marqués, F. Martín, and M. Sorolla, "Babinet principle applied to the design of metasurfaces and metamaterials," *Phys. Rev. Lett.*, Vol. 93, 197401-404, 2004.
6. Falcone, F., T. Lopetegi, J. D. Baena, R. Marqués, F. Martín, and M. Sorolla, "Effective negative  $\epsilon$  stop-band microstrip lines based on complementary split ring resonators," *IEEE Microw. Wireless Compon. Lett.*, Vol. 14, 280–282, Jun. 2004.
7. Baena, J. D., J. Bonache, F. Martín, R. Marqués, F. Falcone, T. Lopetegi, M. A. G. Laso, J. García-García, I. Gil, M. Flores, and M. Sorolla, "Equivalent circuit models for split ring resonators and complementary split ring resonators coupled to planar transmission lines," *IEEE Trans. Microw. Theory Tech.*, Vol. 53, No. 4, 1451–1461, Apr. 2005.
8. Zhang, J., B. Cui, S. Lin, and X.-W. Sun, "Sharp-rejection low-pass filter with controllable transmission zero using complementary split ring resonators (CSRRs)," *Progress In Electromagnetics Research*, PIER 69, 219–226, 2007.
9. Fan, J.-W., C.-H. Liang, and X.-W. Dai, "Design of cross-coupled dual-band filter with equal-length split-ring resonators," *Progress In Electromagnetics Research*, PIER 75, 285–293, 2007.
10. Dai, X.-W., C.-H. Liang, B. Wu, and J. Fan, "Novel dual-band bandpass filter design using microstrip open-loop resonators," *Journal of Electromagnetic Waves and Applications*, Vol. 22, No. 2, 219–225, 2008.
11. Li, C., K.-Y. Liu, and F. Li, "Design of microstrip highpass filters with complementary split ring resonators," *Electronics Letters*, Vol. 43, No. 1, 35–36, 2007.
12. Kim, J., C. S. Cho, and J. W. Lee, "5.2 GHz notched ultra wideband antenna using slot type SRR," *Electronics Letters*, Vol. 42, No. 6, 315–316, 2006.
13. Bonache, J., I. Gil, J. García-García, and F. Martín, "New microstrip filters based on complementary split rings resonators," *IEEE Trans. Microw. Theory Tech.*, Vol. 54, No. 1, 265–271, Jan. 2006.
14. Bonache, J., F. Martín, I. Gil, J. García-García, and M. Sorolla, "Microstrip bandpass filters with wide bandwidth and compact dimensions," *Microw. Opt. Technol. Lett.*, Vol. 46, 343–346, Aug. 2005.
15. García-García, J., F. Martín, F. Falcone, J. Bonache, I. Gil, T. Lopetegi, M. A. G. Laso, M. Sorolla, and R. Marqués, "Spurious passband suppression in microstrip coupled line band

- pass filters by means of splir ring resonators,” *IEEE Microw. Wireless Compon. Lett.*, Vol. 14, No. 9, 416–418, Sept. 2004.
16. García-García, J., F. Martín, E. Amat, F. Falcone, J. Bonache, I. Gil, T. Lopetegi, M. A. G. Laso, A. Marcotegui, M. Sorolla, and R. Marqués, “Microwave filters with improved stop band based on sub-wavelength resonators,” *IEEE Trans. Microw. Theory Tech.*, Vol. 53, No. 6, 1997–2006, Jun. 2005.
  17. Collin, R. E., *Field Theory of Guided Waves*, 2nd Edition, IEEE Press, US, 1991.
  18. Hong, J.-S. and M. J. Lancaster, *Microstrip Filters for RF/Microwave Applications*, 2nd Edition, John Wiley & Sons, Inc., Hoboken, New Jersey, Dec. 2001.
  19. Bonache, J., M. Gil, I. Gil, J. García-García, and F. Martin, “On the electrical characteristics of complementary metamaterial resonators,” *IEEE Microwave Wireless Compon Lett.*, Vol. 16, 543–545, 2006.
  20. Trade mark of Zealand Corp.